A neutron diffraction study of the superionic transition in $(Ca_{1-x}Y_x)F_{2+x}$ with $x = 0.06$



1997 J. Phys.: Condens. Matter 9 845

(http://iopscience.iop.org/0953-8984/9/4/005)

J. Phys.: Condens. Matter **9** (1997) 845–857. Printed in the UK PII: S0953-8984(97)75679-0

# A neutron diffraction study of the superionic transition in $(Ca_{1-x}Y_x)F_{2+x}$ with $x = 0.06$

M Hofmann†, S Hull†, G J McIntyre‡ and C C Wilson†

† ISIS Facility, Rutherford Appleton Laboratory, Chilton, Didcot OX11 0QX, UK
‡ Institut Laue–Langevin, BP156, 38042 Grenoble, France

Received 24 June 1996, in final form 28 October 1996

**Abstract.** We have investigated the high-temperature superionic transition of the anion-excess fluorite $(Ca_{1-x}Y_x)\ F_{2+x}$ with $x = 0.06$ using both monochromatic and time-of-flight Laue single-crystal neutron diffraction. The measured Bragg intensities indicate that the cuboctahedral defect clusters found at ambient temperature start to break up into smaller fragments even below the superionic transition temperature, $T_c \sim 1200$ K. Information concerning the local defect configuration at $T = 1173$ K has been provided by modelling the measured distribution of the coherent elastic diffuse scattering within the $(1\bar{1}0)$ plane of reciprocal space. The high-temperature defects are of the 'Willis' type and strongly resemble the short-lived Frenkel clusters found in the pure fluorites such as $CaF_2$ above $T_c$.

## 1. Introduction

Compounds with the fluorite crystal structure provide one of the simplest examples of fast-ion conductors. At a temperature $T_c$ (of order $0.8T_m$, where $T_m$ is the melting temperature) fluorite compounds such as $CaF_2$ undergo a broad transition to the fast-ion phase [1]. The insulating→superionic transition involves no change in lattice symmetry and can be classified as a type II transition in the notation of Boyce and Huberman [2]. The onset of superionic behaviour is characterized by a rapid increase in the ionic conductivity, associated with the onset of dynamic disorder within the anion sublattice, and a λ-type anomaly in the specific heat $C_p$. Neutron scattering studies of the fluorite structured compounds $CaF_2$, $SrCl_2$ and $\beta$-$PbF_2$ have shown that Frenkel disorder dominates in the superionic phase, with short-lived ($\sim 10^{-12}$ s) defect clusters which comprise anion vacancies and interstitials and cause relaxations of the surrounding anion sublattice [3].

The addition of trivalent cations such as $Y^{3+}$ to pure fluorite compounds such as $CaF_2$ is known to increase the low-temperature ionic conductivity and to substantially depress the transition temperature $T_c$ [4]. Technological interest in solid electrolytes has led to considerable research effort aimed at understanding this effect and resolving the structural changes which accompany doping. It is widely accepted that the dopant cations sit substitutionally on the host cation sites and extra anions are accommodated into the fluorite lattice to maintain overall electrical neutrality. However, at significant dopant levels ($\gtrsim$ 1 mol%) discrete defect clusters are formed and detailed descriptions of the disorder within the anion sublattice are only available for a limited number of these 'anion-excess' fluorites. One such compound is $(Ca_{1-x}Y_x)F_{2+x}$ with $x = 0.06$. By combined analysis of the neutron Bragg and diffuse scattering it was shown that the ambient-temperature

0953-8984/97/040845+13$19.50  

structure comprized of randomly distributed cuboctahedral clusters, of the type found in several ordered anion-excess compounds and illustrated in figure 1 [5]. This defect is formed by the conversion of six edge-sharing fluorite cubes into six corner-sharing square antiprisms, accommodating four additional excess anions into the fluorite lattice. The effect of $Y^{3+}$ doping on the superionic transition temperature is also known, with $T_c$ falling from 1430 K (pure $CaF_2$) to $\sim$ 1200 K ($CaF_2$ doped with 6 mol% $Y^{3+}$ [4]). In this work we extend our neutron diffraction study of this compound to investigate the behaviour of these defect clusters as a function of temperature up to 1423 K, to shed light on the profound effects which doping has on the transition temperature.

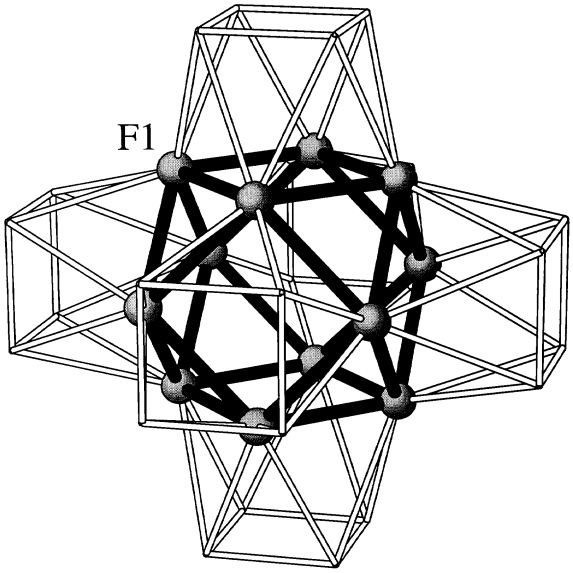


**Figure 1.** A schematic diagram of the cuboctahedral defect cluster found in $(Ca_{1-x}Y_x)F_{2+x}$ with $x = 0.06$ at ambient temperature [5]. The anions which form the cuboctahedron are labelled F1 (see text) and, for clarity, the lattice anions and cations are not shown.

## 2. Experimental details

The neutron scattering experiments were performed on two fragments of a single-crystal boule of $(Ca_{1-x}Y_x)F_{2+x}$ with $x = 0.06$ grown from the melt by Dr R C C Ward of the Clarendon Laboratory Crystal Growth Group, University of Oxford. To avoid excessive extinction of the diffracted beam a small cylindrical crystal of approximately 3 mm diameter and 9 mm length was used to measure the Bragg intensities. The distribution of the relatively weak coherent scattering features observed elsewhere in reciprocal space was measured using a larger crystal of approximately 12 mm diameter and 25 mm length. Both crystals were the same as used in our previously reported study at ambient temperature [5].

The two crystals were aligned and mounted with the $[1\bar{1}0]$ crystallographic axis vertical. Bragg intensity data were collected out to a maximum $h^2+k^2+l^2 = 68$ on the single-crystal diffractometer D10 at the Institut Laue–Langevin (ILL), Grenoble [6]. The diffractometer was operated in its two-circle mode using neutrons of nominal wavelength 1.26 Å. The sample was held by a niobium mount and suspended in a standard ILL neutron beam furnace.

This device surrounds the sample in a resistive heating cylindrical element constructed of niobium, which is in turn enclosed within a series of concentric heat shields constructed of vanadium, chosen because its coherent scattering cross-section for neutrons is very small. Measurements were made at five different temperatures between 293 and 1423 K. The intensity of each reflection was obtained by integrating over $\omega$–$2\theta$ scans, composed of 30 points. The counting time per point varied from 8 to 82 s, depending on the intensity of the reflection. The lattice parameter, $a_0$, was determined at each temperature from the alignment procedure. The values of $a_0$ are summarized in table 1.

**Table 1.** The temperature variation of the lattice parameter $a_0$ of $(Ca_{1-x}Y_x)F_{2+x}$ with $x = 0.06$.

| Temperature (K) | $a_0$ (Å) |
|---|---|
| 293 | 5.498(8) |
| 773 | 5.517(4) |
| 973 | 5.568(4) |
| 1223 | 5.623(3) |
| 1423 | 5.669(4) |

In addition to the Bragg intensity measurements, a measurement of the distribution of the coherent diffuse scattering within the $(1\bar{1}0)$ plane of reciprocal space at 1173 K was performed on the time-of-flight single-crystal diffractometer SXD at the ISIS neutron spallation source. Details of this instrument and its operation were described in our previous publication [5].

## 3. Results

The fluorite crystal structure (space group $Fm\bar{3}m$) can be viewed as a simple cubic array of anions on the 8c Wyckoff sites at $(\frac{1}{4}, \frac{1}{4}, \frac{1}{4})$ etc, with alternate cube centres occupied by cations in 4a sites at $(0, 0, 0)$ etc (see figure 2). Extensive studies of anion-excess fluorite compounds have identified a number of plausible crystallographic sites in which the charge compensating anions can be accommodated (for full details and references see [5]). At low dopant levels ($< 1$ mol% ) these interstitials occupy empty cube centre 4b sites at $(\frac{1}{2}, \frac{1}{2}, \frac{1}{2})$ etc though there is no conclusive evidence that this site is significantly occupied at higher dopant levels. Instead, the excess anions are accommodated in two types of interstitial sites denoted by F(1) and F(2), displaced in the (011) and (111) directions from the empty cube centres. These are situated in Wyckoff sites 48i at $(\frac{1}{2}, u, u)$ with $u \approx 0.38$ and 32f at $(v, v, v)$ with $v \approx 0.40$, respectively.

A number of defect cluster models have been proposed in the literature to explain the relative occupation of such sites. The cuboctahedral clusters observed at ambient temperature in $(Ca_{1-x}Y_x)F_{2+x}$ with $x = 0.06$ accommodate the extra anions in F(1) sites, with no occupancy of F(2) positions. In contrast, clusters formed by single cation-centred antiprisms have occupancy of both F(1) and F(2) sites [7], as do 'Willis' type clusters [8]. The latter can be considered as static counterparts to the Frenkel defect clusters observed in pure fluorites above $T_c$ (see figure 3). A common feature of all these defect clusters is the presence of significant relaxation of surrounding lattice anions toward empty cube centres. These relaxed sites are termed F(3) and are situated in 32f at $(w, w, w)$ with $w \approx 0.29$.

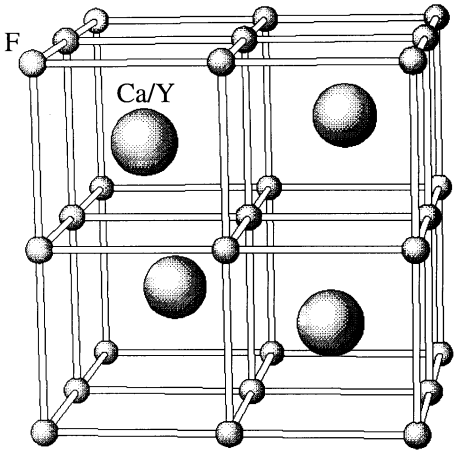


**Figure 2.** A schematic diagram of the fluorite crystal structure showing the anion (F) and cation (Ca/Y) positions.

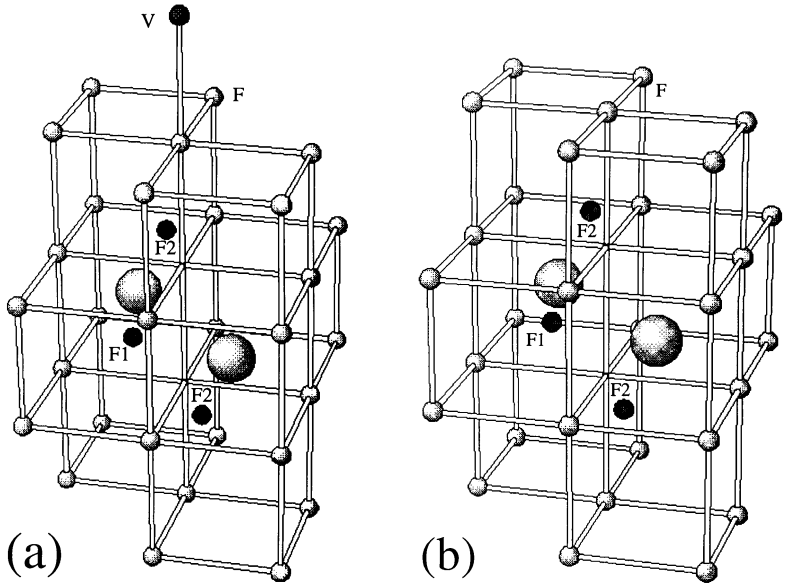


**Figure 3.** Schematic diagrams of (a) the Frenkel defect cluster observed in pure fluorites above the superionic transition temperature [3] and (b) the 'Willis' type defect cluster observed in several anion-excess fluorites at ambient temperature [8, 12]. The large spheres represent the cations (Ca/Y) and the smaller ones the anions. The lighter-shaded anions are occupied lattice sites (F) and the darker ones represent the interstitials (F1) and nearest neighbour relaxed anions (F2). The predicted position of the charge compensating vacancy (V) for the Frenkel cluster based on static energy calculations [15] is also shown.

### *3.1. Bragg diffraction*

Least-squares refinements against the observed Bragg intensity data were undertaken in space group $Fm\bar{3}m$, using the coherent neutron scattering lengths of $b_{Ca} = 4.90$ fm,

$b_Y = 7.75$ fm and $b_F = 5.65$ fm [9]. The cation sites were assumed to be randomly occupied by Ca and Y in the ratio 0.94:0.06 given by the chemical composition. Initial refinements varied only a scale factor, a correction factor for extinction and separate thermal vibration parameters for the cations and the anions. The atoms were constrained to vibrate isotropically. Subsequent analysis allowed the $F^-$ anions to occupy disordered sites F(1) $(\frac{1}{2}, u, u)$ and F(2) $(v, v, v)$. Diffraction studies of $CaF_2$ [10], $BaF_2$ [11] and $SrF_2$ [12] have shown that at elevated temperatures it is necessary to consider anharmonic thermal vibrations of the regular site anions within the fluorite lattice. This vibrational anisotropy is a consequence of the lack of inversion symmetry at the $F^-$ sites at $(\frac{1}{4}, \frac{1}{4}, \frac{1}{4})$, which leads to a greater average amplitude of thermal vibration in the direction of the empty cube centre sites. Consequently, no attempt was made to refine the site occupancy of the relaxed F(3) sites as, for the time-averaged structure determined by Bragg diffraction, they are difficult to distinguish from anharmonic thermal vibrations of the regular site anions. No significant further improvement of the fit was obtained by introducing independent thermal parameters for each type of anion. The main results of the refinement are summarized in table 2, showing the thermal evolution of the final site occupancies, clearly indicating an increase in the occupancy of F(2) sites with increasing temperature.

**Table 2.** Temperature variation of the occupancies of the F(1) and F(2) sites obtained by analysis of the Bragg diffraction data.

| Temperature (K) | F(1) occupancy | F(2) occupancy |
|---|---|---|
| 293 | 0.145(6) | — |
| 773 | 0.10(1) | 0.06(1) |
| 973 | 0.09(4) | 0.07(3) |
| 1223 | 0.11(3) | 0.24(3) |
| 1423 | 0.17(3) | 0.29(5) |

To obtain more precise information concerning the relative site occupancies within the superionic phase a more extensive data set was collected on the SXD diffractometer at 1173 K. In this case the Bragg intensities are measured as a function of incident neutron wavelength, which requires that the Bragg intensities be corrected for extinction prior to the least-squares refinements. The final values of the fitted structural and thermal parameters obtained from simultaneously refining all the site occupancies are given in table 3. The agreement between the observed and calculated Bragg intensities is demonstrated in table 4.

At 1173 K the significant observed occupancy of the F(2) site is clearly incompatible with the existence of cuboctahedral clusters, in which the additional anions are accommodated entirely in F(1) positions. This implies that the cuboctahedral clusters present at ambient temperature break up even below $T_c$. Furthermore, the ratio between the occupancies of the F(1) and F(2) sites is close to 1:2, suggesting the presence of 'Willis' type clusters (figure 3). However, on a more cautious note, previous studies of anion-excess fluorites have discussed possible misinterpretations of such occupancies, since the presence of scattering density associated with the F(2) sites at $\sim (v, v, v)$ can arise from the overlap of the three F(1) peaks at $(\frac{1}{2}, u, u)$, $(u, \frac{1}{2}, u)$ and $(u, u, \frac{1}{2})$ [13]. In view of this possible uncertainty in the interpretation of the Bragg diffraction results we proceed to a detailed analysis of the coherent diffuse scattering measured in the SXD experiment. As discussed previously [5], this approach can give important information on the structure of individual defect clusters, since it directly probes the correlations between disordered ions. In contrast,

**Table 3.** Structural and thermal vibration parameters of $(Ca_{1-x}Y_x)F_{2+x}$ with $x = 0.06$ at $T = 1173$ K determined by least-squares refinement of the Bragg intensities.

| Atom | Site | Position | Parameter |
|---|---|---|---|
| Ca, Y | 4a | (0, 0, 0) | $B_{iso} = 4.3(1)$ Å$^2$ |
| F | 8c | $(\frac{1}{4}, \frac{1}{4}, \frac{1}{4})$ | $B_{iso} = 4.5(2)$ Å$^2$ |
| | | | occ $= 1.75(5)$ |
| F(1) | 48i | $(\frac{1}{2}, u, u)$ | $B_{iso} = 4.5(2)$ Å$^2$ |
| | | | occ $= 0.10(2)$ |
| | | | $u = 0.391(12)$ |
| F(2) | 32f | $(v, v, v)$ | $B_{iso} = 4.5(2)$ Å$^2$ |
| | | | occ $= 0.21(2)$ |
| | | | $v = 0.341(4)$ |

**Table 4.** A comparison between the calculated intensities of the Bragg peaks, $I_{calc}(hkl)$, using the structural parameters listed in table 3, and the observed intensities measured at 1173 K on SXD, $I_{obs}(hkl)$, which have estimated standard deviation $\sigma I_{obs}(hkl)$.

| *hkl* | $I_{obs}(hkl)$ | $\sigma I_{obs}(hkl)$ | $I_{calc}(hkl)$ |
|---|---|---|---|
| 002 | 252.2 | 26.9 | 257.6 |
| 004 | 632.1 | 32.2 | 675.4 |
| 008 | 17.4 | 2.9 | 17.4 |
| 026 | 108.4 | 2.7 | 104.2 |
| 044 | 204.7 | 9.5 | 215.1 |
| 066 | 15.5 | 4.1 | 10.7 |
| 113 | 178.9 | 10.3 | 164.8 |
| 115 | 46.9 | 1.5 | 43.7 |
| 117 | 11.4 | 1.1 | 7.7 |
| 133 | 75.5 | 2.2 | 62.1 |
| 135 | 25.5 | 1.4 | 29.4 |
| 137 | 5.6 | 1.1 | 4.7 |
| 155 | 7.1 | 1.4 | 7.3 |
| 222 | 97.7 | 6.2 | 96.1 |
| 224 | 363.9 | 11.1 | 387.0 |
| 228 | 9.7 | 2.4 | 9.7 |
| 246 | 39.3 | 3.8 | 33.8 |
| 333 | 88.1 | 5.8 | 67.5 |
| 335 | 9.4 | 1.2 | 9.9 |
| 355 | 9.6 | 2.2 | 5.7 |
| 444 | 61.8 | 4.6 | 61.5 |

analysis of the Bragg scattering data alone gives only the time-averaged occupation of the unit cell, averaged over the whole crystal.

### *3.2. Diffuse scattering*

Figure 4 shows the distribution of the coherent diffuse scattering in the $(1\bar{1}0)$ plane of reciprocal space measured at $T = 1173$ K. The distribution of intensity is markedly different from that observed at ambient temperature [5], with broader features and the majority of the scattering concentrated at relatively low values of scattering vector. The method of analysis which has been adopted here uses the comparison of the measured diffuse scattering intensities with that calculated using assumed models for the defect clusters. Initially, such

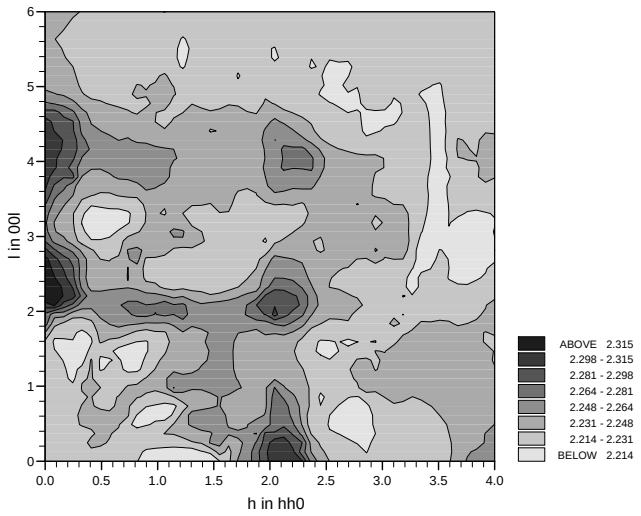


**Figure 4.** The coherent diffuse scattering distribution in the $(1\bar{1}0)$ plane measured from the $(Ca_{1-x}Y_x)F_{2+x}$ sample with $x = 0.06$ at 1173 K.

comparisons are made visually, with the aim of selecting only those models which appear suitable candidates for more detailed (and time consuming) analysis. Having identified good starting models to describe the measured diffuse scattering, the structural parameters describing the defect can be optimized by least-squares minimization of the usual $\chi^2$ statistic, defined by

$$\chi^2 = \sum_{N_d} \frac{(I(\boldsymbol{Q})_{obs} - I(\boldsymbol{Q})_{calc})^2}{(\sigma I(\boldsymbol{Q})_{obs})^2} / (N_d - N_p).$$

$I(\boldsymbol{Q})_{obs}$ and $I(\boldsymbol{Q})_{calc}$ are the measured and calculated diffuse scattering at each scattering vector position $\boldsymbol{Q}$ and $\sigma I(\boldsymbol{Q})_{obs}$ is the estimated standard deviation of $I(\boldsymbol{Q})_{obs}$ and is derived from the counting statistics. $N_d$ is the number of data points ($\boldsymbol{Q}$ positions) used in the fit and $N_p$ is the number of fitted parameters.

For the initial calculations (figures 5–8) the position and thermal vibration parameters are taken from the analysis of the Bragg scattering listed in table 3. As might be expected, the cuboctahedral cluster model gives a relatively poor agreement between the calculated and measured diffuse scattering data, as shown in figure 5. Laval and Frit [7] have suggested a series of defect clusters which can be derived by conversion of a single $(Ca, Y)F_8$ fluorite cube into a square antiprism. This produces four anions on F(1) sites and four vacancies on regular lattice anion sites. Four different clusters of this type are proposed, by incorporating between one and four excess anions along (111) directions in the F(2) sites. Such clusters can be viewed as fragments of the larger cuboctahedral clusters but, despite their being a plausible possibility, the calculated pattern (figure 6) indicates that they must be discounted.

'Willis' type clusters were found to account satisfactorily for the diffuse neutron scattering from $B_{1-x}La_xF_{2+x}$ [14] and $UO_{2.13}$ [8] at elevated temperature and, as illustrated in figure 3, are similar to the Frenkel clusters formed in pure $CaF_2$ above $T_c$. The simplest cluster of the 'Willis' type is the 2:1:2 cluster, where the notation vacancies:true interstitials:relaxed anions is used. The true interstitial, at an F(1) site displaced by $(x, \bar{x}, 0)$ from the centre of the cube edge, causes two nearest neighbours to relax along (111) towards

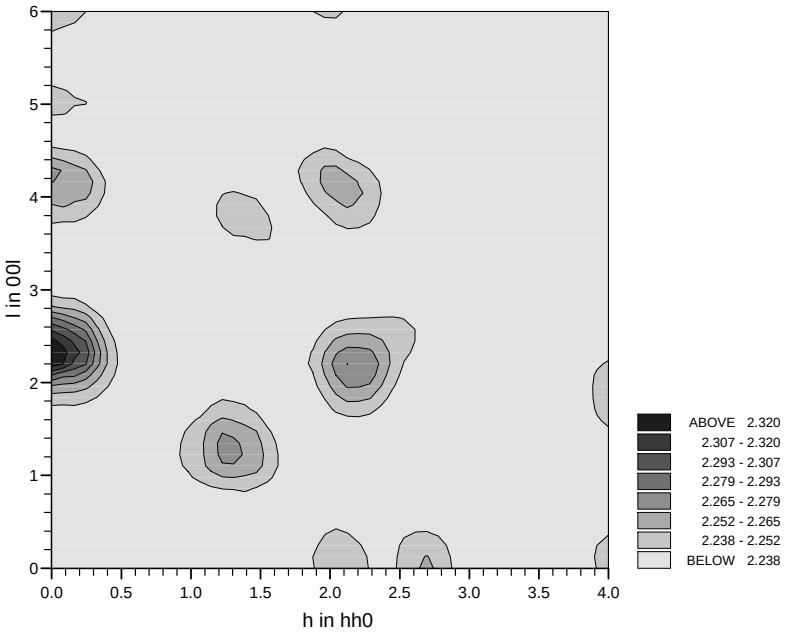


**Figure 5.** The calculated diffuse scattering distribution in the $(1\bar{1}0)$ plane assuming a random distribution of cuboctahedral type defect clusters.

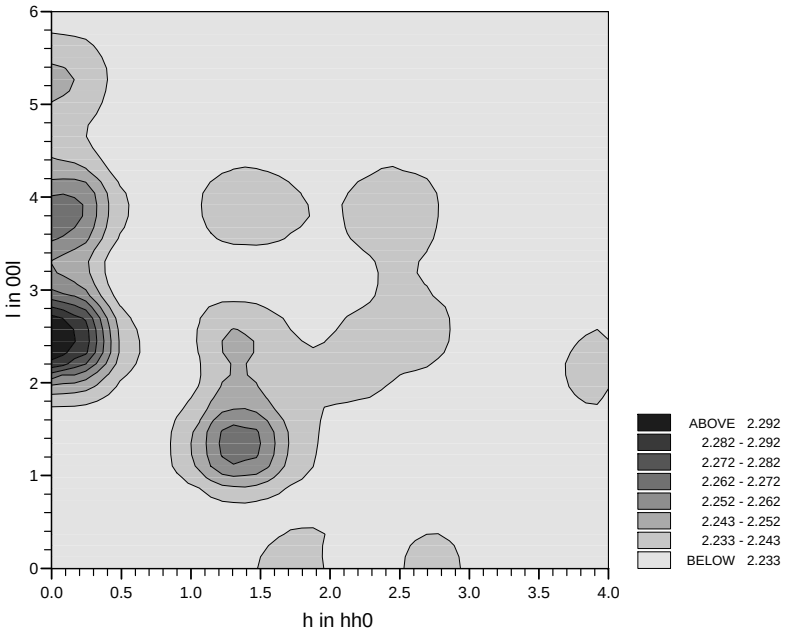


**Figure 6.** The calculated diffuse scattering distribution in the $(1\bar{1}0)$ plane assuming a random distribution of square antiprism defect clusters of the type proposed by Laval and Frit [7].

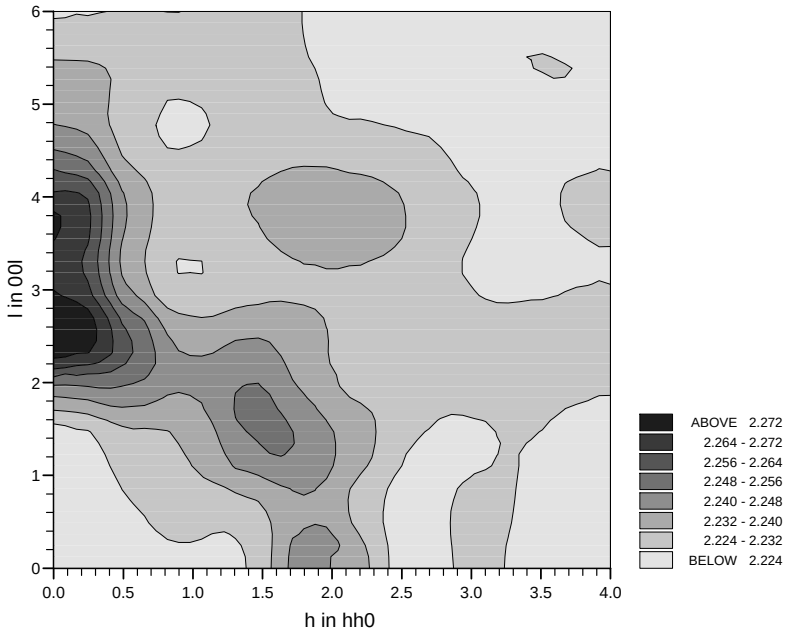


**Figure 7.** The calculated diffuse scattering distribution in the $(1\bar{1}0)$ plane assuming a random distribution of 2:1:2 type defect clusters.

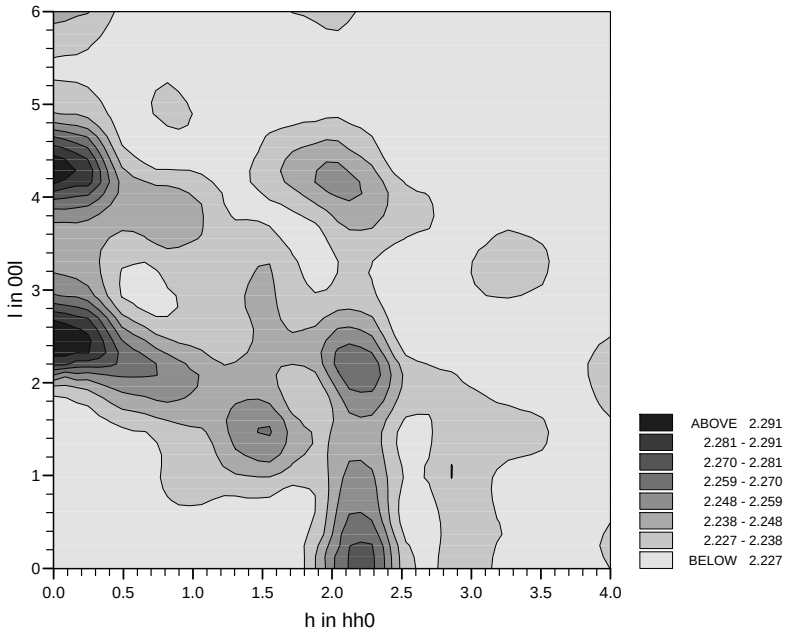


**Figure 8.** The calculated diffuse scattering distribution in the $(1\bar{1}0)$ plane assuming a random distribution of 8:1:8 'Willis' type defect clusters.

empty cube centres (see figure 3). The 2:2:2 cluster is a 2:1:2 cluster supplemented by an extra true interstitial which occupies the symmetrical site displaced by $(\overline{x}, x, 0)$ to form an interstitial pair. In both the 2:1:2 and 2:2:2 clusters the relaxed anions in F(2) sites cause the six next-nearest-neighbour anions to relax towards adjacent empty cube centres, to avoid anomalously short $F^-$–$F^-$ distances. This produces 8:1:8 and 8:2:8 clusters, respectively. Calculations based on the smaller clusters (2:1:2 and 2:2:2) generate diffuse peaks which are roughly in the expected regions of $\boldsymbol{Q}$ space, though somewhat broader than those measured (figure 7). The additional relaxation of the surrounding lattice in 8:1:8 and 8:2:8 clusters produces longer-range correlations between disordered anions and provides the required narrowing of the diffuse features in reciprocal space. The 8:1:8 case is slightly better than the 8:2:8 and its calculated pattern is shown in figure 8.

The encouraging results using the 'Willis' type clusters above suggest that we also consider the intrinsic Frenkel defects found in the fast-ion phase of pure fluorites. In the notation used above, this corresponds to a 9:1:8 cluster, since charge balance relies on the presence of a thermally activated interstitial–vacancy pair, rather than a dopant–interstitial mechanism. The general distribution of calculated diffuse scattering is very similar to that obtained using the 8:1:8 cluster. For the particular defect model considered here, it appears, therefore, that the distribution of diffuse scattering is relatively insensitive to the location of the charge compensating vacancy. Trial simulations using different vacancy sites confirmed this finding and, as a result, the vacancy is assumed to adopt the position predicted by static energy calculations [15]. Similarly, trial calculations showed that the diffuse scattering is insensitive to the positions of the dopant cations relative to the anion interstitials and these were included in the calculations or least-squares fits to the data.

Least-squares fits to the diffuse scattering data were performed using the 8:1:8 and 9:1:8 clusters, with starting values taken from the Bragg scattering analysis. In both cases $N_p = 8$, comprising a scale factor, two background parameters (one $\boldsymbol{Q}$ independent and one linearly related to $|\boldsymbol{Q}|$) plus positional and isotropic thermal vibration parameters for each of the three anion types (F(1), F(2) and F(3)). The least-squares procedure produced little improvement to the quality of fit in either case and the difference between the values of the goodness-of-fit parameter cannot be considered significant ($\chi^2 = 10.4$ and 9.1 for the 8:1:8 and 9:1:8 clusters, respectively). The refined values of the positional and thermal vibration

**Table 5.** A comparison between values of the positional and thermal vibration parameters obtained from least-squares analysis of the Bragg and coherent diffuse scattering data of $(Ca_{1-x}Y_x)F_{2+x}$ with $x = 0.06$ at 1173 K. For comparison, the data used in the interpretation of diffuse scattering from pure $CaF_2$ close to the superionic transition [3] are also given.

| | | $(Ca_{1-x}Y_x)F_{2+x}$ $x = 0.06$ (this work) | | $CaF_2$ [3] |
|---|---|---|---|---|
| Atom | Position | Bragg | Diffuse (8:1:8) | Diffuse (9:1:8) |
| F(1) | $(\frac{1}{2}, u, u)$ | $B_{iso} = 4.5(2)$ Å$^2$ | $B_{iso} = 6.6(9)$ Å$^2$ | $B_{iso} = 7.0$ Å$^2$ |
| | | $u = 0.391(12)$ | $u = 0.387(3)$ | $u = 0.36$ |
| F(2) | $(v, v, v)$ | $B_{iso} = 4.5(2)$ Å$^2$ | $B_{iso} = 5.9(5)$ Å$^2$ | $B_{iso} = 7.0$ Å$^2$ |
| | | $v = 0.341(4)$ | $v = 0.349(8)$ | $v = 0.40$ |
| F(3) | $(w, w, w)$ | — | $B_{iso} = 4.5(2)$ Å$^2$ | $B_{iso} = 7.0$ Å$^2$ |
| | | — | $w = 0.287(2)$ | $w = 0.31$ |
| | $N_p$ | 7 | 8 | — |
| | $N_d$ | 41 | 2301 | — |
| | $\chi^2$ | 2.7 | 10.4 | — |

parameters are also the same for each model, within the experimental uncertainty on the fitted values. However, the agreement between the values obtained by independent analysis of the Bragg and diffuse scattering (illustrated in table 5 for the 8:1:8 case) strongly supports our assumption earlier in this paper that the dominant defect clusters in $Ca_{1-x}Y_xF_{2+x}$ with $x = 0.06$ close to $T_c$ are of this type. The distinction between 'Willis' type 8:1:8 clusters and 'Frenkel' type 9:1:8 clusters will be addressed further in the following section.

## 4. Discussion

Table 5 also compares the values of positional and thermal vibrational parameters obtained in this work for $Ca_{1-x}Y_xF_{2+x}$ with $x = 0.06$ close to $T_c$ with the corresponding values used in the interpretation of data from $CaF_2$ using 9:1:8 clusters [3]. No estimates of the uncertainties in the values of $u$, $v$ and $w$ are given in [3] and it appears unwise to speculate on possible physical significance of the apparent differences between the values of $u$, $v$ and $w$ for doped and undoped systems.

At a temperature of 1173 K we have shown that the observed Bragg and diffuse scattering can be modelled in a successful, and consistent, manner on the assumption of 8:1:8 and/or 9:1:8 clusters. Whilst our experimental data are not of sufficient quality to differentiate between these two defect models some general observations can be made. We begin by re-analysing the Bragg diffraction data at each temperature but with explicit constraints imposed to reduce the number of fitted parameters and, as a result, to obtain more reliable values for the numbers of defects. It is important to note, however, that these constraints are supported by the independent analysis of the diffuse scattering. We consider only two defect models, the cuboctahedral and the 8:1:8/9:1:8 type, and fix the positional parameters $u$, $v$ and $w$ at the values found at ambient temperature [5] and 1173 K (table 3). The occupancies of the F(1), F(2) and F(3) sites are also constrained to be in the ratios 1:0:2 and 1:2:6 for the cuboctahedral and 8:1:8/9:1:8 clusters, respectively. However, we do not explicitly include a lattice site vacancy for the latter (since we cannot at this stage differentiate between the 8:1:8 and 9:1:8 models) though the overall constraint of charge neutrality is retained.

The reanalysis of the Bragg data uses six fitted parameters; a scale factor, an extinction correction parameter, a single isotropic thermal parameter for both the cations and anions and two defect concentration parameters. The latter are expressed as the number of defects (cuboctahedral or 8:1:8/9:1:8 type) per unit cell and are illustrated in figure 9. At the lowest (ambient) temperature the concentration of cuboctahedral defects is 0.059(3), in good agreement with the value of 0.06 expected if these are the only type of defect present. It is clear, however, that the number of cuboctahedral defects decreases at temperatures well below $T_c$, such that the majority of these clusters have broken up prior to the superionic transition. Such behaviour is perhaps to be expected, since the presence of such large, and presumably immobile, defects is not conducive to enhanced ionic conductivity of the type observed in the doped compound.

The number of 8:1:8/9:1:8 clusters increases steadily and has a value of $\sim 0.21$/unit cell at temperatures around $T_c$. If all the excess anions in the $(Ca_{1-x}Y_x)F_{2+x}$ sample form 8:1:8 clusters then the number of defects per unit cell would be $4x$, i.e. 0.24. It would appear, therefore, that extrinsic defects (8:1:8) caused by the addition of trivalent $Y^{3+}$ dominate at the superionic transition and the extent of thermally induced intrinsic Frenkel disorder (9:1:8) is rather small. Indeed, figure 9 includes the corresponding estimates of the extent of Frenkel disorder (9:1:8 clusters) in $CaF_2$ [3]. In the pure compound there is a significant number of Frenkel defects per unit cell ($\sim 0.2$) and the level of intrinsic disorder is higher than in the doped case, even though the latter has a higher ionic conductivity at $T_c$. From

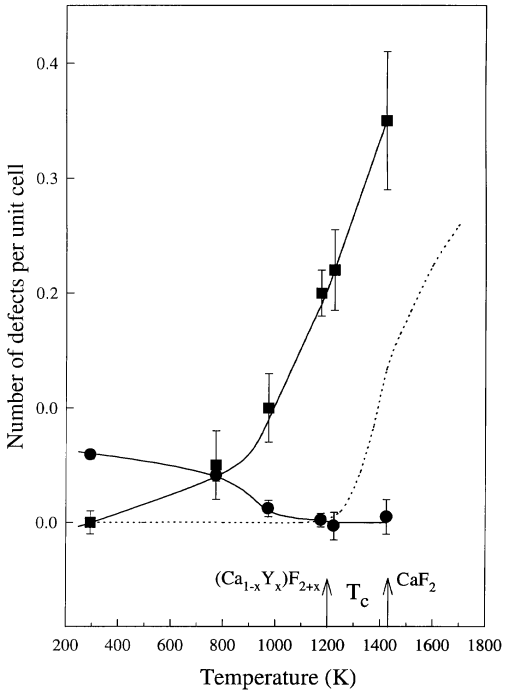


**Figure 9.** The temperature variation of the number of cuboctahedral defect clusters per unit cell (●) and the number of 8:1:8/9:1:8 type clusters per unit cell (■) present in $(Ca_{1-x}Y_x)F_{2+x}$ with $x = 0.06$. The solid lines are guides to the eye. The dotted line is an estimate of the corresponding number of 9:1:8 type clusters observed in pure $CaF_2$ [3].

this we conclude that the extrinsic 8:1:8 clusters must be dynamic in nature and contribute to the high anion mobility.

At the highest temperature measured in this study (1423 K) the uncertainties in the defect concentrations are somewhat larger though the number of 8:1:8/9:1:8 clusters per unit cell ($\sim 0.35$) is now far higher than can be accounted for by the excess anions introduced by doping despite the larger uncertainties in the defect concentrations. At this temperature there must therefore be a larger degree of intrinsic disorder than at lower temperatures.

## 5. Conclusions

The defect structure of the anion-excess fluorite $(Ca_{1-x}Y_x)F_{2+x}$ with $x = 0.06$ has been investigated by single-crystal neutron diffraction studies to 1423 K. The cuboctahedral defect clusters formed at ambient temperature are found to break up on increasing temperature. At the superionic transition temperature ($T_c \sim 1200$ K) the observed high ionic conductivity arises from dynamic clusters of the 'Willis' type, which have a strong structural relationship to the Frenkel clusters found in the superionic phase of pure $CaF_2$ [3]. Above $T_c$, both 'Willis' and 'Frenkel' type clusters are present, with both contributing to the ionic diffusion process.

Finally, this work emphasizes the importance of combined analysis of both the Bragg and coherent diffuse scattering for studies of systems containing significant concentrations

of defects. The presence of extensive disorder is characterized by extremely high thermal vibration parameters and the resultant rapid fall-off in Bragg scattering with increasing $\boldsymbol{Q}$ limits the number of independent reflections which can be measured. Analysis of the diffuse scattering, which probes short-range correlations between disordered ions, provides independent confirmation of the defect geometry and allows more reliable values of the position and thermal vibration parameters of the interstitial and relaxed ions to be obtained. Using this information to constrain the analysis of the Bragg scattering can then give better estimates of the site occupancies and, as a result, more reliable values for the concentrations of the defects present.

## Acknowledgments

We are grateful to Dr R C C Ward of the Crystal Growth Group, Clarendon Laboratory, University of Oxford, for preparing the single-crystal samples used in this work.

## References

[1] Hayes W 1980 *J. Physique Coll.* **41** C6 7
[2] Boyce J B and Huberman B A 1979 *Phys. Rep.* **51** 1
[3] Hutchings M T, Clausen K, Dickens M H, Hayes W, Kjems J K, Schnabel P G and Smith C 1984 *J. Phys. C: Solid State Phys.* **17** 3903
[4] Catlow C R A, Comins J D, Germano F A, Harley R T, Hayes W and Owen I B 1981 *J. Phys. C: Solid State Phys.* **14** 329
[5] Hull S and Wilson C C 1992 *J. Solid State Chem.* **100** 101
[6] Ibel K (ed) 1994 *Guide to Neutron Research Facilities at the ILL* (Grenoble: Institut Laue–Langevin)
[7] Laval J P and Frit B 1983 *J. Solid State Chem.* **49** 237
[8] Willis B T M and Hazell R G 1980 *Acta Crystallogr.* A **36** 582
[9] Koestler L and Yelon W B 1982 *Summary of Low Energy Neutron Scattering Lengths and Cross Sections* (Petten: Netherlands Research Foundation Department of Physics)
[10] Willis B T M 1965 *Acta Crystallogr.* **18** 75
[11] Cooper M J and Rouse K D 1968 *Acta Crystallogr.* A **24** 405
[12] Forsyth J B, Wilson C C and Sabine T M 1989 *Acta Crystallogr.* A **45** 244
[13] Muradyan L A, Maksimov B A, Aleksandrov V B, Otroshchenko L P, Bydanov N N, Sirota M I and Simonov V I 1986 *Sov. Phys.–Crystallogr.* **31** 390
[14] Andersen N H, Clausen K and Kjems J K 1983 *Solid State Ion.* **9/10** 543
[15] Catlow C R A and Hayes W 1982 *J. Phys. C: Solid State Phys.* **15** L9